PROCEEDINGS OF SCIENCE

Lattice computation of the second order transport coefficient κ in Yang-Mills theory

O. Philipsen, C. Schäfer*
Institut für Theoretische Physik, Goethe-Universität Frankfurt,
Max-von-Laue Str. 1, 60438 Frankfurt am Main, Germany
E-mail: philipsen, cschaefer@th.physik.uni-franfurt.de

From heavy-ion collision experiments we know that the quark-gluon plasma behaves almost like an ideal fluid and can be described by hydrodynamics. The dynamic properties of the quark-gluon plasma are determined by transport coefficients.
The second order transport coefficient κ is related to a momentum expansion of the Euclidean energy-momentum tensor correlator at vanishing Matsubara frequency. This allows the determination of κ from first principles without maximum entropy methods. We present the results obtained by pure Yang-Mills lattice simulations in comparison to a computation in leading-order lattice perturbation theory as well as the temperature dependence of the transport coefficient κ.

31st International Symposium on Lattice Field Theory - LATTICE 2013
July 29 - August 3, 2013
Mainz, Germany

*Speaker.

PoS(LATTICE 2013)177

1. Introduction

One of the major findings of the experimental heavy ion programme [1–4] is that QCD matter at high temperatures and low densities behaves as a nearly ideal fluid with very low viscosity. This conclusion is based on the fact that experimental data are excellently described by relativistic hydrodynamics, with transport coefficients fitted to the data [5]. Unfortunately, theoretical predictions of transport coefficients from the fundamental theory QCD remain very difficult. An exception to this conceptual difficulty is the second-order hydrodynamic coefficient κ [6, 7], which can be related to Euclidean correlation functions through Kubo formulae. Here we present a first attempt to determine κ from the momentum expansion of a suitable two-point function in a lattice simulation.

2. The transport coefficient κ

2.1 Relativistic hydrodynamics

The basic quantity in relativistic hydrodynamics is the energy momentum tensor which can be decomposed into an ideal part $T_0^{\mu\nu}$ and a dissipative part $\Pi^{\mu\nu}$

$$T^{\mu\nu} = T^{\mu\nu}_{(0)} + \Pi^{\mu\nu}, \qquad \Pi^{\mu\nu} = \pi^{\mu\nu} + (g^{\mu\nu} + u^\mu u^\nu)\,\Pi. \tag{2.1}$$

The dissipative contribution consists of a traceless part $\pi^{\mu\nu}$ and a part with non-vanishing trace Π. The former has been specified for a non-conformal fluid in a second order gradient expansion in $N = 4$ Super-Yang-Mills theory [7]

$$\pi^{\mu\nu} = -\eta\,\sigma^{\mu\nu} + \eta\,\tau_\pi \left(\langle D\sigma^{\mu\nu} \rangle + \frac{\nabla \cdot u}{3}\sigma^{\mu\nu} \right) + \kappa \left(R^{\langle\mu\nu\rangle} - 2u_\alpha u_\beta R^{\alpha\langle\mu\nu\rangle\beta} \right) + \dots \,. \tag{2.2}$$

The kinetic coefficients are identified as transport coefficients. Besides the shear viscosity η and the relaxation time τ_π, to second order the transport coefficient κ enters the expansion and couples to the symmetrized Riemann curvature tensor R, its contractions and the fluid's four velocity u^μ.

2.2 Thermal field theory

For the computation of the transport coefficient κ from QCD a relation between its definition in relativistic hydrodynamics and quantum field theory is necessary. This can be achieved by considering the fluid's linear response to a metric perturbation and establishes a connection between the transport coefficient κ and the low momentum behaviour of the retarded thermal correlator of the energy momentum tensor [6]. In the case of vanishing frequency retarded and Euclidean correlator coincide [8] and one finds

$$G^{\mathrm{E}}(\omega = 0, \vec{q}) = G'(0) + \frac{\kappa}{2}|\vec{q}|^2 + \mathscr{O}(|\vec{q}|^4), \tag{2.3}$$

$$G^{\mathrm{E}}(x,y) = \langle T_{12}(x) T_{12}(y) \rangle \,. \tag{2.4}$$

The transport coefficient κ can now be obtained as the slope of the low momentum correlator $G^{\mathrm{E}}(q^2)$. It has been determined in a low momentum expansion in pure gluodynamics in the ideal gas limit, i.e. at vanishing coupling [9, 10],

$$\kappa = (N_{\mathrm{c}} - 1)\,\frac{T^2}{18}. \tag{2.5}$$

Remarkably, the transport coefficient κ has an non-vanishing value in flat spacetime, although it is the kinetic coefficient in front of the Riemann curvature tensor in its definition from $N = 4$ Super-Yang-Mills theory (2.2).

3. Computation of κ in lattice QCD

3.1 Lattice framework

We employ Wilson's Yang-Mills action on an anisotropic lattice implying different lattice spacings in temporal and spatial direction, a_σ and a_τ, respectively,

$$S[U] = \frac{\beta}{N_\mathrm{c}} \mathrm{Re}\,\mathrm{Tr}\left[\frac{1}{\xi_0}\sum_{x,i<j}(1-U_{ij}(x)) + \xi_0 \sum_{x,i}(1-U_{i0}(x))\right] \tag{3.1}$$

with lattice coupling $\beta = 2N_\mathrm{c}/g^2$, plaquette variables $U_{\mu\nu}$ and bare anisotropy ξ_0. Quantum fluctuations cause a deviation of the actual anisotropy $\xi = a_\sigma/a_\tau$. The two are related by a renormalisation factor $\eta(\beta,\xi) = \xi/\xi_0(\beta,\xi)$, whose numerical evaluation we take from [11]. The scale is set for a specific value of the anisotropy, $\xi = 2$, by means of the string tension [12].

As will be discussed in section 3.4 the discretised energy-momentum tensor requires multiplicative renormalisation due to reduced translational invariance on the lattice. Regarding the renormalisation procedure it is favourable to express the correlator (2.4) in terms of diagonal elements instead of nondiagonal ones. We establish this by the so called cubic symmetry [13]

$$\langle T_{12}(x)T_{12}(y)\rangle = \frac{1}{2}\Big[\langle T_{11}(x)T_{11}(y)\rangle - \langle T_{11}(x)T_{22}(y)\rangle\Big]. \tag{3.2}$$

Additionally, temporal and spatial elements of the energy-momentum tensor require separate renormalisation factors Z_τ and Z_σ on an anisotropic lattice. The diagonal energy-momentum tensor elements in the clover discretisation [14] read

$$a_\sigma^3 a_\tau \mathrm{T}_{ii}(x) = \frac{\beta}{128N_\mathrm{c}} \mathrm{Re}\,\mathrm{Tr}\,[Z_\tau(\beta,\xi)T_{ii}^\tau(x) + Z_\sigma(\beta,\xi)T_{ii}^\sigma], \tag{3.3}$$

where

$$T_{ii}^\tau(x) = \xi_0 \widehat{F}_{0i}^2(x) - \xi_0 \sum_{k\neq i} \widehat{F}_{k0}^2(x), \tag{3.4a}$$

$$T_{ii}^\sigma(x) = -\frac{1}{\xi_0}\sum_{\substack{k,j\neq i\\ k<j}} \widehat{F}_{kj}^2(x) + \frac{1}{\xi_0}\sum_k \widehat{F}_{ki}^2(x). \tag{3.4b}$$

3.2 Connection of κ to lattice QCD

In order to extract the transport coefficient κ we compute the correlator (2.3) within the lattice framework presented in section 3.1

$$a_\sigma^3 a_\tau G^\mathrm{E}(q_3) = \frac{1}{V}\sum_{x,y} \mathrm{e}^{-\mathrm{i}q_3(x_3-y_3)} \langle T_{12}(x)T_{12}(y)\rangle\,. \tag{3.5}$$

The definition of the transport coefficient κ relies on a small momentum expansion of the correlator. We identify temperature as the relevant scale for comparison with the momenta and demand $q_i/T < 1$. With the discretised versions of temperature $T = 1/(a_\tau N_\tau)$ and momenta $q_i = 2\pi/(a_\sigma N_\sigma) n_i$ with $n_i = 0, 1, \ldots, N_\sigma - 1$ we find for the ratio on the lattice

$$\frac{q_i}{T} = \frac{2\pi N_\tau}{\xi N_\sigma} n_i < 1. \tag{3.6}$$

The temporal lattice extent N_τ is fixed by the temperature. In order to extract the transport coefficient κ by performing a linear fit of equation (2.3), the number of momenta obeying the constraint (3.6) should be larger than three. Thus the simulation requires large spatial lattice extents N_σ, which makes the calculation costly. This can be partly remedied by working with anisotropic lattices $\xi > 1$.

3.3 Computation of κ in lattice perturbation theory

In order to estimate lattice artefacts and check our numerics and renormalisation procedure, we compute the transport coefficient κ from lattice perturbation theory. This is done on an anisotropic lattice with anisotropy ξ in the case of vanishing coupling ($g = 0$). We find by expansions in the lattice spacing and momentum for the correlator (2.3)

$$\begin{aligned}\frac{G^E(q)}{T^4} = (N_c^2 - 1)\Bigg\{ &\frac{\pi^4}{N_\tau^2}\left(\frac{2\xi^2}{945} + \frac{4}{189}\right) \\ &+ \frac{q^2}{T^2}\left[\frac{1}{36} + \frac{\pi^2}{N_\tau^2}\left(-\frac{\xi^2}{240} + \frac{49}{2160}\right)\right]\Bigg\} + \mathcal{O}\left(q^4, N_\tau^{-4}\right),\end{aligned} \tag{3.7}$$

from which we identify the transport coefficient κ as

$$\frac{\kappa}{T^2} = (N_c^2 - 1)\left[\frac{1}{18} + \frac{\pi^2}{N_\tau^2}\left(-\frac{\xi^2}{120} + \frac{49}{1080}\right)\right] + \mathcal{O}\left(q^4, N_\tau^{-4}\right). \tag{3.8}$$

3.4 Renormalisation procedure

The correlator defined in (2.4) suffers from ultraviolet divergences. We correct the correlator by additive renormalisation, i.e. subtracting the vacuum part. We define a new vacuum corrected expectation value by $\langle \mathcal{O} \rangle = \langle \mathcal{O} \rangle_T - \langle \mathcal{O} \rangle_0$, where $\langle \mathcal{O} \rangle_T$ is an observable evaluated at a given temperature T and $\langle \mathcal{O} \rangle_0$ its vacuum contribution, i.e. evaluated at vanishing temperature.

Discretisation of spacetime also requires a multiplicative renormalisation, since the energy-momentum tensor is the Noether-current corresponding to translational invariance and translations only form a discrete symmetry group on the lattice. On an anistropic lattice the renormalisation factor depends on the lattice coupling β and the anisotropy ξ. Additionally, temporal and spatial direction require separate renormalisation. It is favourable to rewrite the energy-momentum tensor as

$$T_{ii}^{\mathrm{R}} = Z_\tau(\beta, \xi)\left[T_{ii}^\tau + \frac{Z_\sigma(\beta, \xi)}{Z_\tau(\beta, \xi)} T_{ii}^\sigma\right]. \tag{3.9}$$

Performing the renormalisation procedure we need the ratio $Z_\sigma(\beta, \xi_0)/Z_\tau(\beta, \xi_0)$ and the absolute scale $Z_\tau(\beta, \xi_0)$. The former can be obtained by renormalisation group invariant quantities [15],

Run	β	N_τ	N_σ	N_τ^{vac}	ξ	a_σ [fm]	$T^{\mathrm{vac}}/T_{\mathrm{c}}$	$T^{\mathrm{vac}}/T_{\mathrm{c}}$
i	7.1	6	120	72	2	0.026	9.4	0.8
ii	7.1	8	120	72	2	0.026	7.1	0.8
iii	6.68	6	120	42	2	0.044	5.6	0.8
iv	6.14	6	120	24	2	0.094	2.6	0.7

Table 1: Simulation parameters for four evaluations of κ. The lower temperature T^{vac} is required for renormalisation.

the latter by utilising the physical interpretation of the energy-momentum tensor. The diagonal spatial elements are equivalent to the pressure $\left\langle T_{ii}^{\mathrm{R}}\right\rangle_0 = p$, where we use the continuum extrapolated pressure from the lattice. We determine the absolute renormalisation constant by matching the energy-momentum tensor computed from the lattice [16] with the continuum pressure at the same temperatures.

4. Numerical results

4.1 Comparison to lattice perturbation theory

Our first simulation aims at reproducing the free lattice peturbation theory result of the transport coefficient κ from section 3.3. The running coupling allows to reach the weak coupling regime in lattice QCD by increasing the temperature. Thus we simulate at $T = 9.4\,T_{\mathrm{c}}$ with with $T_{\mathrm{c}} \approx 260\,\mathrm{MeV}$ for pure Yang-Mills theory [17]. The complete simulation parameters can be found in row (i) in table 1.

Figure 1 shows the correlator $G^{\mathrm{E}}(q)/T^4$ for five momenta compared to the result from lattice perturbation theory. Fitting the datapoints of the correlator to a linear function yields for the transport coefficient $\kappa/T^2 = 0.40(26)$, which agrees with the lattice perturbation theory result $\kappa_{\mathrm{LPT}}/T^2 = 0.47$. An exact agreement is not yet expected since at $T = 9.4\,T_{\mathrm{c}}$ we entered rather the weak coupling regime than the free theory regime. Thus the lattice perturbation theory result for the transport coefficient κ suffers from the missing next-to-leading order corrections and their lattice artefacts.

4.2 Temperature dependence

In principle, the temperature can be varied at fixed β and lattice spacing by changing N_τ, where lower temperature implies larger N_τ. However, due to the constraint on the momenta from equation (3.6) this would require a similar increase of the spatial volume and thus a drastical growth of the numerical effort. Hence the fixed scale approach is not practical for temperatures approaching the phase transition.

We therefore investigate the temperature dependence of κ at fixed N_τ/N_σ by repeating the simulations at various lattice couplings β. In this case the different temperatures are evaluated at different lattice spacings, and consequently also different spatial volumes in physical units. However, since our lattice spacings are all $a_\sigma < 0.1\,\mathrm{fm}$, we expect the lattice artefacts on the temperature dependence of the transport coefficient κ/T^2 to be negligible. As a consistency check for this, we

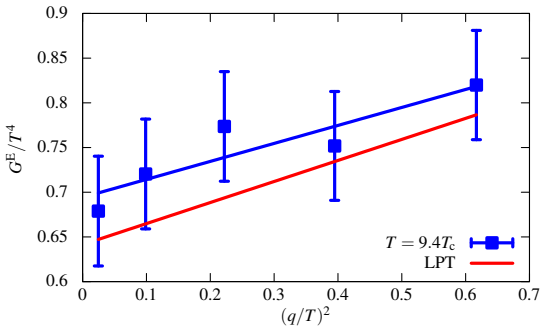

Figure 1: $G^{\mathrm{E}}(q)/T^4$ for momenta $q^2/T^2 < 1$ compared to results from lattice perturbation theory (LPT). The slope of the linear fit gives $\kappa/2$.

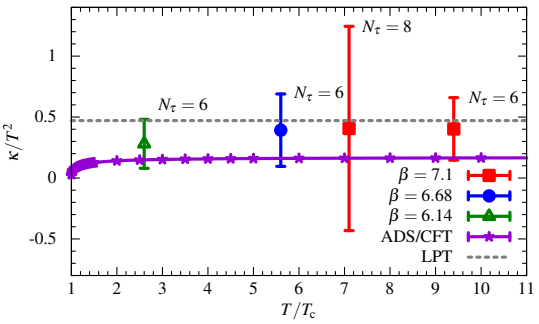

Figure 2: Temperature dependence of the transport coefficient κ/T^2 compared to ADS/CFT correspondence and lattice perturbation theory.

T/T_c	9.4	7.1	5.6	2.6
a_σ [fm]	0.026	0.026	0.044	0.094
κ/T^2	0.40(26)	0.41(84)	0.39(30)	0.28(20)

Table 2: Lattice results for the transport coefficient κ/T^2 at different spatial lattice spacings a_σ and temperatures T/T_c.

also perform simulations at different temperatures but the same lattice spacings (simulations (i) and (ii) in table 1).

The results are shown in figure 2. The datapoint at $T = 7.1\,T_c$ suffers from large errorbars since the spatial lattice extents have been kept fixed while increasing the temporal lattice extent N_τ. Because of the constraint (3.6) this corresponds to slightly larger momenta and generates a loss of accuracy in the fit. Within the errorbars, the values of κ/T^2 at $T = 9.4\,T_c$ and $T = 7.1\,T_c$ agree and thus justify the comparison at different lattice spacings and temperatures.

The numerical values for the transport coefficient κ are also summarised in table 2. Within errorbars, the temperature dependence of the transport coefficient is consistent with that of the ideal gas, $\kappa \sim T^2$, which is also the prediction of ADS/CFT [6]. Assuming this functional dependence we may increase accuracy by averaging the data points with $N_\tau = 6$ to give our final result,

$$\kappa^{\mathrm{avr}} = 0.36(15)T^2. \tag{4.1}$$

Because of still large errorbars, our result also quantitatively covers both the leading order perturbative as well as the AdS/CFT prediction rescaled by the lattice QCD entropy [16]. This would suggest that, besides improved simulation methods, next-to-leading order analytic calculations should be able to give a result with improved accuracy.

Acknowledgments

C. S. is supported by the Helmholtz International Center for FAIR within the LOEWE program of the State of Hesse. C.S. acknowledges travel support by the Helmholtz Research School H-QM.

The calculations have been performed on LOEWE-CSC. The authors thank the LOEWE-CSC team for support.

References

[1] K. Adcox et al. Formation of dense partonic matter in relativistic nucleus-nucleus collisions at RHIC: Experimental evaluation by the PHENIX collaboration. *Nucl.Phys.*, A757:184–283, 2005. doi: 10.1016/j.nuclphysa.2005.03.086.

[2] B.B. Back, M.D. Baker, M. Ballintijn, D.S. Barton, B. Becker, et al. The PHOBOS perspective on discoveries at RHIC. *Nucl.Phys.*, A757:28–101, 2005. doi: 10.1016/j.nuclphysa.2005.03.084.

[3] I. Arsene et al. Quark gluon plasma and color glass condensate at RHIC? The Perspective from the BRAHMS experiment. *Nucl.Phys.*, A757:1–27, 2005. doi: 10.1016/j.nuclphysa.2005.02.130.

[4] John Adams et al. Experimental and theoretical challenges in the search for the quark gluon plasma: The STAR Collaboration's critical assessment of the evidence from RHIC collisions. *Nucl.Phys.*, A757:102–183, 2005. doi: 10.1016/j.nuclphysa.2005.03.085.

[5] Ulrich W Heinz and Raimond Snellings. Collective flow and viscosity in relativistic heavy-ion collisions. *Annu. Rev. Nucl. Part. Sci.*, 63:123–151, 2013. doi: 10.1146/annurev-nucl-102212-170540.

[6] R. Baier, Romatschke, P., Son, D. T., Starinets, A. O., and Stephanov, M. A. Relativistic viscous hydrodynamics, conformal invariance, and holography. *JHEP*, 04:100, 2008. doi: 10.1088/1126-6708/2008/04/100.

[7] P. Romatschke. Relativistic Viscous Fluid Dynamics and Non-Equilibrium Entropy. *Class. Quant. Grav.*, 27:025006, 2010. doi: 10.1088/0264-9381/27/2/025006.

[8] Harvey B. Meyer. Transport Properties of the Quark-Gluon Plasma: A Lattice QCD Perspective. *Eur.Phys.J.*, A47:86, 2011. doi: 10.1140/epja/i2011-11086-3.

[9] P. Romatschke and Son, D. T. Spectral sum rules for the quark-gluon plasma. *Phys.Rev.*, D80:065021, 2009. doi: 10.1103/PhysRevD.80.065021.

[10] Guy D. Moore and Kiyoumars A. Sohrabi. Thermodynamical second-order hydrodynamic coefficients. *JHEP*, 1211:148, 2012. doi: 10.1007/JHEP11(2012)148.

[11] Timothy R. Klassen. The Anisotropic Wilson gauge action. *Nucl.Phys.*, B533:557–575, 1998. doi: 10.1016/S0550-3213(98)00510-0.

[12] Y. Namekawa et al. Thermodynamics of SU(3) gauge theory on anisotropic lattices. *Phys.Rev.*, D64: 074507, 2001. doi: 10.1103/PhysRevD.64.074507.

[13] F. Karsch and H.W. Wyld. Thermal Green's Functions and Transport Coefficients on the Lattice. *Phys.Rev.*, D35:2518, 1987. doi: 10.1103/PhysRevD.35.2518.

[14] Martin Luscher, Stefan Sint, Rainer Sommer, and Peter Weisz. Chiral symmetry and O(a) improvement in lattice QCD. *Nucl.Phys.*, B478:365–400, 1996. doi: 10.1016/0550-3213(96)00378-1.

[15] Harvey B. Meyer. Energy-momentum tensor correlators and viscosity. *PoS*, LATTICE2008:017, 2008.

[16] Sz. Borsanyi, G. Endrodi, Z. Fodor, S.D. Katz, and K.K. Szabo. Precision SU(3) lattice thermodynamics for a large temperature range. *JHEP*, 1207:056, 2012. doi: 10.1007/JHEP07(2012)056.

[17] G. Boyd et al. Thermodynamics of SU(3) Lattice Gauge Theory. *Nucl. Phys.*, B469:419–444, 1996. doi: 10.1016/0550-3213(96)00170-8.